PHYSICAL REVIEW C, VOLUME 65, 064004

Spin dependent momentum distributions of proton-deuteron clusters in ^{3}He from electron scattering on polarized ^{3}He: Theoretical predictions

J. Golak,[1,2] W. Glöckle,[1] H. Kamada,[3] H. Witała,[2] R. Skibiński,[2] and A. Nogga[4]
[1]*Institut für Theoretische Physik II, Ruhr Universität Bochum, D-44780 Bochum, Germany*
[2]*M. Smoluchowski Institute of Physics, Jagiellonian University, PL-30059 Kraków, Poland*
[3]*Department of Physics, Faculty of Engineering, Kyushu Institute of Technology, 1-1 Sensuicho, Tobata, Kitakyushu 804-8550, Japan*
[4]*Department of Physics, University of Arizona, Tucson, Arizona 85721*
(Received 21 February 2002; published 28 May 2002)

The process $\overrightarrow{^3\mathrm{He}}(e,e'\vec{p})d$ [or $\overrightarrow{^3\mathrm{He}}(e,e'\vec{d})p$] is studied theoretically in a Faddeev treatment with the aim to have access to the spin dependent momentum distribution of $\vec{p}\vec{d}$ clusters in polarized ^{3}He. Final state interactions and meson exchange currents turn out to have a strong influence in the considered kinematical regime (below the pion threshold). This precludes direct access to the momentum distribution except for small deuteron momenta. Nevertheless, the results for the longitudinal and transverse response functions are interesting as they reflect our present day understanding of the reaction mechanism and therefore data would be very useful.

DOI: 10.1103/PhysRevC.65.064004 PACS number(s): 21.45.+v, 24.70.+s, 25.10.+s, 25.40.Lw

I. INTRODUCTION

With knowledge of solving precisely few-nucleon equations, the availability of high-precision nucleon-nucleon (NN) potentials and insight into the electromagnetic nucleonic current operator it is seducing to ask very detailed questions about spin dependent momentum distributions inside light nuclei and the way to access them through electron scattering taking final state interactions fully into account. Momentum distributions of polarized $\vec{d}\vec{p}$ clusters in spin-oriented ^{3}He have been studied before; see, for instance, [1]. We address here the question whether these distributions are accessible through the $\overrightarrow{^3\mathrm{He}}(e,e'\vec{p})d$ or $\overrightarrow{^3\mathrm{He}}(e,e'\vec{d})p$ processes. Optimal kinematical conditions are that the polarizations of ^{3}He and of the knocked out proton (deuteron) and the momenta of the final proton and deuteron are collinear to the photon momentum. As we will show the longitudinal and transverse response functions will lead, up to known factors, directly to the sought spin dependent momentum distribution of the $\vec{p}\vec{d}$ clusters in ^{3}He. One can also define a proper asymmetry, which carries corresponding information. Of course this can only be true in a plane-wave impulse approximation (PWIA) and for the absorption of the photon on a single nucleon. Rescattering effects in the final state as well as meson exchange currents (MECs) will disturb the outcome. The strength of that disturbance again will depend on the photon momentum Q with the hope that it decreases with increasing Q.

We formulate the electromagnetic process in Sec. II and also display there the $\vec{p}\vec{d}$ cluster momentum distributions of ^{3}He. Section III shows our results for the $\overrightarrow{^3\mathrm{He}}(e,e'\vec{p})d$ and $\overrightarrow{^3\mathrm{He}}(e,e'\vec{d})p$ processes based on the AV18 NN potential [2] and precise solutions of the corresponding Faddeev equations. Since our predictions depend on the full dynamics in a highly nontrivial manner, a future experimental verification will be an important test for the understanding of few-nucleon dynamics. We end with a brief summary in Sec. IV.

II. THEORY

The spin dependent momentum distribution of proton-deuteron clusters inside the ^{3}He nucleus is defined as

$$\mathcal{Y}(M,M_d,m;\vec{q}_0) \equiv \langle \Psi M \| \phi_d M_d\rangle \left| \vec{q}_0 \frac{1}{2} m \right\rangle \left\langle \vec{q}_0 \frac{1}{2} m \right| \langle \phi_d M_d \| \Psi M\rangle, \tag{1}$$

where $\vec{q}_0$ is the proton momentum (the deuteron momentum is $-\vec{q}_0$); m, M_d, and M are spin magnetic quantum numbers for the proton, deuteron, and the considered nucleus, respectively.

We introduce our standard basis in momentum space [3]

$$|pq\alpha\rangle \equiv \left| pq(ls)j\left(\lambda \frac{1}{2}\right)J\mathcal{J}M\left(t\frac{1}{2}\right)TM_T\right\rangle, \tag{2}$$

where p and q are magnitudes of Jacobi momenta and the set of discrete quantum numbers α comprises angular momenta, spins, and isospins for a three-nucleon ($3N$) system. Then $\mathcal{Y}(M,M_d,m;\vec{q}_0)$ can be evaluated as

$$\mathcal{Y}(M,M_d,m;\vec{q}_0) = \Bigg| \sum_\alpha (\delta_{l0}+\delta_{l2})\delta_{s1}\delta_{j1}\delta_{t0} C\left(1I\frac{1}{2};M_d,\ M-M_d,M\right) \times C\left(\lambda\frac{1}{2}I;M-M_d-m,m,M-M_d\right) \times \int_0^\infty dp\, p^2 \phi_l(p)\langle pq_0\alpha|\Psi\rangle Y^\star_{\lambda,M-M_d-m}(\hat{q}_0)\Bigg|^2. \tag{3}$$

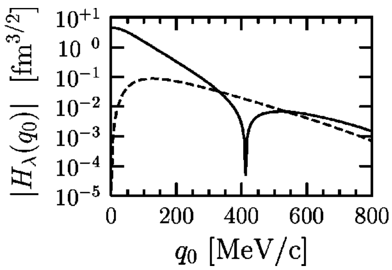

FIG. 1. Absolute value of $H_\lambda(q_0)$ defined in Eq. (5) for $\lambda=0$ (solid line) and $\lambda=2$ (dashed line). Note $H_0(q_0)<0$ for $q_0>400$ MeV/c, while $H_2(q_0)$ remains always positive for the shown q_0 values.

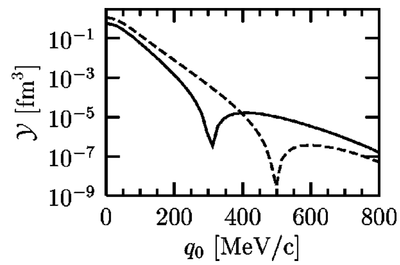

FIG. 2. Spin dependent momentum distributions $\mathcal{Y}(M=\frac{1}{2},\ M_d=0,\ m=\frac{1}{2};|\vec{q}_0|\hat{z})$ (solid line) and $\mathcal{Y}(M=\frac{1}{2},\ M_d=1,\ m=-\frac{1}{2};|\vec{q}_0|\hat{z})$ (dashed line) for $\vec{p}\vec{d}$ clusters in ^{3}He.

In Eq. (3), $\langle pq_0\alpha|\Psi\rangle$ are the partial-wave projected wave function components of ^{3}He in momentum space and $\phi_l(p)$ are the s- and d-wave components of the deuteron.

Further we rewrite $\mathcal{Y}(M,M_d,m;\vec{q}_0)$ as

$$\mathcal{Y}(M,M_d,m;\vec{q}_0) = \left|\sum_{\lambda=0,2} Y_{\lambda,M-M_d-m}(\hat{q}_0)C\left(1I_\lambda\frac{1}{2};M_d,M-M_d,M\right) \times C\left(\lambda\frac{1}{2}I_\lambda;M-M_d-m,m,M-M_d\right) \times \sum_{l=0,2}\int_0^\infty dp\,p^2\phi_l(p)\langle pq_0\alpha_{l\lambda}|\Psi\rangle\right|^2. \quad (4)$$

and define an auxiliary quantity $H_\lambda(q_0)$ as

$$H_\lambda(q_0)\equiv\sum_{l=0,2}\int_0^\infty dp\,p^2\phi_l(p)\langle pq_0\alpha_{l\lambda}|\Psi\rangle,\quad \lambda=0,2. \quad (5)$$

Note that the set $\alpha_{l\lambda}$ contributes only for the deuteron quantum numbers $s=1$, $j=1$, and $t=0$. Further $I_\lambda=\frac{1}{2}$ for $\lambda=0$ and $\frac{3}{2}$ for $\lambda=2$. It is clear that using this quantity $H_\lambda(q_0)$ the spin dependent momentum distribution $\mathcal{Y}(M,M_d,m;\vec{q}_0)$ can be constructed for any combination of magnetic quantum numbers and direction $\hat{q}_0$.

In this paper all our calculations are based on the NN force AV18 [2]. We display $H_\lambda(q_0)$ in Fig. 1. Note that λ is the relative orbital angular momentum of the proton with respect to the deuteron inside ^{3}He. As we see from Fig. 1, the s wave ($\lambda=0$) dominates the momentum distribution $\mathcal{Y}$ for the small relative momenta and has a node around $q_0=400$ MeV/c. Near that value and above the s- and d-wave contributions are comparable.

In Fig. 2 we show the quantities $\mathcal{Y}(M,M_d,m;\vec{q}_0)$ for $\vec{q}_0$ pointing in the direction of the spin quantization axis and the ^{3}He nucleus polarized with $M=1/2$. The polarizations of the proton and deuteron are chosen as $M_d=0$, $m=1/2$ and $M_d=1$, $m=-1/2$, respectively. We see an interesting shift in the minima from $q_0=$ 300 to 500 MeV/c, if the polarization of the proton (deuteron) switches from a parallel (perpendicular) to an antiparallel (parallel) orientation in relation to the spin direction of ^{3}He. This strong spin dependence leads to a pronounced spin asymmetry defined as

$$A\equiv\frac{\mathcal{Y}(M=\frac{1}{2},M_d=0,\ m=\frac{1}{2};|\vec{q}_0|\hat{z})-\mathcal{Y}(M=\frac{1}{2},M_d=1,\ m=-\frac{1}{2};|\vec{q}_0|\hat{z})}{\mathcal{Y}(M=\frac{1}{2},M_d=0,\ m=\frac{1}{2};|\vec{q}_0|\hat{z})+\mathcal{Y}(M=\frac{1}{2},M_d=1,\ m=-\frac{1}{2};|\vec{q}_0|\hat{z})} \quad (6)$$

and shown in Fig. 3.

Next we ask the question how this quantity can be accessed experimentally. The cross section for the process $e+{}^3\mathrm{He}\rightarrow e'+p+d$ has the form [4]

$$\sigma=\sigma_{\mathrm{Mott}}\{(v_LW_L+v_TW_T+v_{TT}W_{TT}+v_{TL}W_{TL}) + h(v_{T'}W_{T'}+v_{TL'}W_{TL'})\}\rho, \quad (7)$$

where σ_{Mott}, v_i, and ρ are analytically given kinematical factors, and h is the helicity of the incoming electron. The response functions W_i, which contain the whole dynamical information, are constructed from the current matrix elements taken between the initial bound state $|\Psi M\rangle$ and the final scattering state $|\Psi_{pd}^{(-)}M_dm\rangle$ [5]. They are given as

$$W_L=|\langle\Psi_{pd}^{(-)}M_dm|j_0(\vec{Q})|\Psi M\rangle|^2\equiv|N_0|^2,$$

$$W_T=|\langle\Psi_{pd}^{(-)}M_dm|j_{+1}(\vec{Q})|\Psi M\rangle|^2 + |\langle\Psi_{pd}^{(-)}M_dm|j_{-1}(\vec{Q})|\Psi M\rangle|^2\equiv|N_{+1}|^2+|N_{-1}|^2,$$

$$W_{TT}=2\,\mathrm{Re}[N_{+1}(N_{-1})^\star],$$

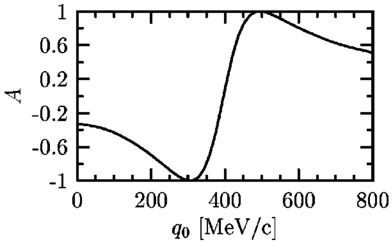

FIG. 3. The asymmetry $A=[\mathcal{Y}(m=\frac{1}{2})-\mathcal{Y}(m=-\frac{1}{2})]/[\mathcal{Y}(m=\frac{1}{2})+\mathcal{Y}(m=-\frac{1}{2})]$.

$$W_{TL}=-2\,\mathrm{Re}[N_0(N_{+1}-N_{-1})^\star],$$

$$W_{T'}=|N_{+1}|^2-|N_{-1}|^2,$$

$$W_{TL'}=-2\,\mathrm{Re}[N_0(N_{+1}+N_{-1})^\star]. \tag{8}$$

Note that $W_{T'}$ and $W_{TL'}$ contribute only in the case when the initial electron is polarized. This is our standard notation N of the nuclear matrix element, where the indices 0 and ± 1 stand for the zeroth component and the transverse spherical components of the current. The general $3N$ current operator contains the single-nucleon contributions as well as two- and three-nucleon exchange terms

$$j_\mu(\vec{Q})=j_\mu(\vec{Q};1)+j_\mu(\vec{Q};2)+j_\mu(\vec{Q};3). \tag{9}$$

In the nonrelativistic limit, which we use, the three contributing pieces of the single-nucleon current operator (the charge density, the convection, and the spin current) can be written in the $3N$ momentum space as

$$j_0(\vec{Q};1)=\int d\vec{p}\int d\vec{q}\,|\vec{p}\vec{q}\rangle\hat{\Pi}(Q)\left\langle \vec{p}\vec{q}-\frac{2}{3}\vec{Q}\right|, \tag{10}$$

$$j_\tau(\vec{Q};1;\mathrm{conv})=\int d\vec{p}\int d\vec{q}\,|\vec{p}\vec{q}\rangle\frac{q_\tau}{m_N}\hat{\Pi}(Q)\left\langle \vec{p}\vec{q}-\frac{2}{3}\vec{Q}\right|, \tag{11}$$

$$j_\tau(\vec{Q};1;\mathrm{spin})=\int d\vec{p}\int d\vec{q}\,|\vec{p}\vec{q}\rangle\frac{Q\tau\sigma_\tau}{2m_N}\hat{\Pi}_M(Q)\left\langle \vec{p}\vec{q}-\frac{2}{3}\vec{Q}\right|, \tag{12}$$

where m_N is the nucleon mass and $\hat{\Pi}(Q)$ and $\hat{\Pi}_M(Q)$ are sums of isospin projection operators for the neutron and proton joined by the electric (G_E) and magnetic (G_M) nucleon form factors, respectively (see [5]). We assumed that $\vec{Q}\|\hat{z}$.

Let us now decompose the scattering state $|\Psi^{(-)}_{pd}M_dm\rangle$ in the following way:

$$|\Psi^{(-)}_{pd}M_dm\rangle\equiv|\phi_dM_d\vec{q}_fm\rangle+|\Psi^{\mathrm{rest}}_{pd}M_dm\rangle. \tag{13}$$

The first term is just a product of the deuteron wave function $|\phi_dM_d\rangle$ and a relative momentum eigenstate of the spectator nucleon $|\vec{q}_fm\rangle$. The other term accounts for the proper antisymmetrization of the final state and all rescattering contributions.

If the many-nucleon contributions to the $3N$ current $[j_\mu(\vec{Q};2)$ and $j_\mu(\vec{Q};3)]$ and $|\Psi^{\mathrm{rest}}_{pd}M_dm\rangle$ can be neglected (PWIA assumption), then the current matrix elements take the following form:

$$N_0^{\mathrm{PWIA}}(M,M_d,m)=G_E(Q)\sum_\alpha(\delta_{l0}+\delta_{l2})\delta_{s1}\delta_{j1}\delta_{t0}C\left(1I\frac{1}{2};M_d,M-M_d,M\right)C\left(\lambda\frac{1}{2}I;M-M_d-m,m,M-M_d\right)$$
$$\times Y_{\lambda,M-M_d-m}\left(\widehat{\vec{q}_f-\frac{2}{3}\vec{Q}}\right)\int_0^\infty dp\,p^2\langle p|\vec{q}_f-\frac{2}{3}\vec{Q}|\alpha|\Psi\rangle\phi_l(p), \tag{14}$$

$$N_\tau^{\mathrm{conv\ PWIA}}(M,M_d,m)=\sqrt{\frac{4\pi}{3}}\frac{q_f}{m_N}Y_{1\tau}(\hat{q}_f)N_0^{\mathrm{PWIA}}(M,M_d,m), \tag{15}$$

$$N_\tau^{\mathrm{spin\ PWIA}}(M,M_d,m)=\frac{\sqrt{3}}{2}\tau\frac{Q}{m_N}G_M(Q)C\left(\frac{1}{2}1\frac{1}{2};m-\tau,\tau,m\right)\sum_\alpha(\delta_{l0}+\delta_{l2})\delta_{s1}\delta_{j1}\delta_{t0}C\left(1I\frac{1}{2};M_d,M-M_d,M\right)$$
$$\times C\left(\lambda\frac{1}{2}I;M-M_d-m+\tau,m-\tau,M-M_d\right)Y_{\lambda,M-M_d-m+\tau}\left(\widehat{\vec{q}_f-\frac{2}{3}\vec{Q}}\right)$$
$$\times\int_0^\infty dp\,p^2\langle p|\vec{q}_f-\frac{2}{3}\vec{Q}|\alpha|\Psi\rangle\phi_l(p). \tag{16}$$

In the laboratory frame $\vec{p}_N+\vec{p}_d=\vec{Q}$ and by definition of the Jacobi momentum $\vec{q}_f=\frac{2}{3}\vec{p}_N-1/3\vec{p}_d$, thus $\vec{q}_f-\frac{2}{3}\vec{Q}=-\vec{p}_d$. The second argument of the ^{3}He wave function component is therefore just the deuteron laboratory momentum. For the parallel kinematics ($\vec{Q}\|\vec{p}_N\|\vec{p}_d$) the matrix element $N_\tau^{\rm conv\ PWIA}$ is zero.

In this particular situation and for the initial target spin parallel to $\vec{Q}$ $(M=\frac{1}{2})$ only few combinations of the magnetic quantum numbers contribute to the nuclear matrix elements $N_0^{\rm PWIA}$ and $N_{\pm 1}^{\rm spin\ PWIA}$. Because of the choice of the parallel kinematics and the property of the spherical harmonics these are $M=\frac{1}{2},M_d=0,m=\frac{1}{2}$ and $M=\frac{1}{2},M_d=1,m=-\frac{1}{2}$ in $N_0^{\rm PWIA}$, $M=\frac{1}{2},M_d=0,m=-\frac{1}{2}$ and $M=\frac{1}{2},M_d=-1,m=\frac{1}{2}$ in $N_{-1}^{\rm spin\ PWIA}$, and $M=\frac{1}{2},M_d=1,m=\frac{1}{2}$ in $N_{+1}^{\rm spin\ PWIA}$.

Furthermore, if we compare the expressions given in Eqs. (14) and (16) to the one in Eq. (3), we find that the spin dependent momentum distributions $\mathcal{Y}$ of ^{3}He are connected to $N_i^{\rm PWIA}$ by

$$\mathcal{Y}\left(M=\frac{1}{2},M_d=0,\ m=\frac{1}{2};|\vec{p}_d|\hat{z}\right)$$
$$=\frac{1}{(G_E)^2}\left|N_0^{\rm PWIA}\left(M=\frac{1}{2},M_d=0,\ m=\frac{1}{2}\right)\right|^2$$
$$=\frac{2m_N^2}{Q^2(G_M)^2}\left|N_{-1}^{\rm spin\ PWIA}\left(M=\frac{1}{2},M_d=0,\ m=-\frac{1}{2}\right)\right|^2 \tag{17}$$

and by

$$\mathcal{Y}\left(M=\frac{1}{2},M_d=1,\ m=-\frac{1}{2};|\vec{p}_d|\hat{z}\right)$$
$$=\frac{1}{(G_E)^2}\left|N_0^{\rm PWIA}\left(M=\frac{1}{2},M_d=1,\ m=-\frac{1}{2}\right)\right|^2$$
$$=\frac{2m_N^2}{Q^2(G_M)^2}\left|N_{+1}^{\rm spin\ PWIA}\left(M=\frac{1}{2},M_d=1,\ m=\frac{1}{2}\right)\right|^2. \tag{18}$$

In the case of parallel kinematics W_{TT}, W_{TL}, and $W_{TL'}$ vanish. This follows from the fact that the conditions on the magnetic quantum numbers, M, M_d, and m, given in products of N_0, N_{+1}, and N_{-1}, cannot be simultaneously fulfilled. For an experiment with unpolarized electrons, the cross section (7) contains then only the longitudinal (W_L) and transverse (W_T) response functions:

$$\sigma=\sigma_{\rm Mott}(v_L W_L+v_T W_T)\rho. \tag{19}$$

Thus the standard "L-T" separation is required in order to access individually W_L and W_T.

Another possibility is offered by an experiment with a polarized electron beam. In this case no further separation of response functions is required, since

$$\frac{1}{2}[\sigma(h=+1)-\sigma(h=-1)]\frac{1}{v_{T'}\rho}=|N_{+1}|^2-|N_{-1}|^2. \tag{20}$$

Therefore under these extreme simplifying assumptions the response functions W_L, W_T, and $W_{T'}$, carry directly the desired information. Note that in case of W_T $(W_{T'})$ only one of the two parts gives a nonzero contribution.

The full dynamics adds antisymmetrization in the final state. [Note our single nucleon current operator as given in Eqs. (10)–(12) acts only on one particle. Antisymmetrization in the final state is equivalent to the action of the current on all three particles.] Then of course rescattering to all orders in the NN t operator has to be included. On top one should add at least two-body currents. We have described how to do that before at several places [5]. Here we only remark that we employ standard π- and ρ-like exchange currents related to the NN force AV18, which we use throughout the paper, and that adequate Faddeev equations for ^{3}He and for the treatment of FSI have been solved precisely.

III. RESULTS

Since we work strictly nonrelativistically we want to keep the $3N$ c.m. energy $E_{3N}^{\rm c.m.}$ below the pion threshold. But in that regime we would like to study many kinematical configurations and also include higher three-momenta Q of the photon. We display in Table I the kinematical conditions, for which our studies have been carried through. In parallel kinematics one can distinguish three cases for the momentum orientations of the final proton and deuteron, which we denote by C_1, C_2, and C_3, and which are depicted in Fig. 4. Thus for C_2 the final momenta of proton and deuteron are parallel to $\vec{Q}$, whereas in C_1 and C_3 only one of them lies in the direction of $\vec{Q}$, the other is opposite. Table I shows for an (arbitrarily selected) initial electron energy of 1.2 GeV various relevant variables: the electron scattering angle, the proton and deuteron momenta p_N and p_d, the photon energy ω, the three-momentum of the photon Q, and finally the $3N$ c.m. energy $E_{3N}^{\rm c.m.}$. The additional label distinguishes the three cases C_1–C_3. We see that for each fixed p_d value we cover a certain range of Q values. The three C_1 configurations with $E_{3N}^{\rm c.m.}>140$ MeV are above the pion threshold and have to be taken with caution. We evaluated all the cases of Table I but do not show all in case the results are similar. Figure 5 displays $W_L/(G_E)^2$ for $M_d=0$, $m=\frac{1}{2}$ and $M_d=1$, $m=-\frac{1}{2}$ against the available Q values according to Table I. According to Eqs. (17) and (18), in the PWIA, $W_L/(G_E)^2$ is just the sought $\mathcal{Y}$ and thus trivially independent of Q. Symmetrizing the final state but still neglecting rescattering is called PWIAS, while predictions including addition-

TABLE I. Electron kinematics together with different kinematical quantities used to extract the spin dependent momentum distributions of proton-deuteron clusters in ^{3}He.

θ_e (deg)	p_N (MeV/c)	p_d (MeV/c)	ω (MeV)	Q (MeV/c)	$E_{3N}^{\mathrm{c.m.}}$ (MeV)	
14.45	310	10	56.67	300	35.22	C_1
19.43	410	10	95.01	400	61.14	C_1
24.56	510	10	144.00	500	94.15	C_1
29.91	610	10	203.63	600	134.26	C_1
35.58	710	10	273.92	700	181.47	C_1
14.21	400	100	93.33	300	71.89	C_1
19.11	500	100	141.26	400	107.38	C_1
24.15	600	100	199.83	500	149.98	C_1
29.39	700	100	269.05	600	199.68	C_1
19.41	200	200	37.44	400	3.56	C_2
24.52	300	200	64.06	500	14.21	C_2
29.85	400	200	101.33	600	31.96	C_2
35.46	500	200	149.25	700	56.81	C_2
41.46	600	200	207.82	800	88.76	C_2
16.93	50	300	30.80	350	3.58	C_2
27.05	250	300	62.74	550	3.58	C_2
29.70	300	300	77.39	600	8.02	C_2
35.22	400	300	114.66	700	22.21	C_2
41.10	500	300	162.58	800	43.51	C_2
21.94	50	400	49.45	450	8.04	C_2
35.06	300	400	96.04	700	3.60	C_2
40.80	400	400	133.32	800	14.25	C_2
14.21	200	500	93.41	300	71.96	C_3
19.47	100	500	77.44	400	43.56	C_3
24.05	10	500	72.17	490	24.08	C_3
13.31	300	600	149.35	300	127.90	C_3
19.28	200	600	122.73	400	88.86	C_3
24.62	100	600	106.76	500	56.91	C_3
29.32	10	600	101.49	590	34.23	C_3

ally final state interactions (FSIs) are denoted by "Full." We see a change of patterns in going from $p_d=100$ to 200 and from 400 to 500 MeV/c. As seen from Table I this is related to the different motions of the final proton and deuteron; in other words, one switches from the configuration C_1 to C_2

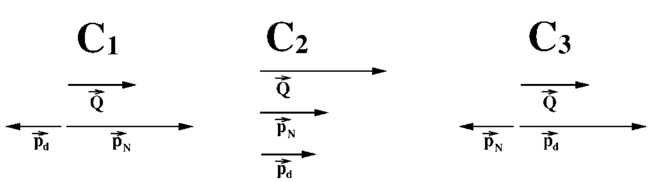

FIG. 4. Three-momenta arrangements C_1, C_2, and C_3 for parallel kinematics. See Table I.

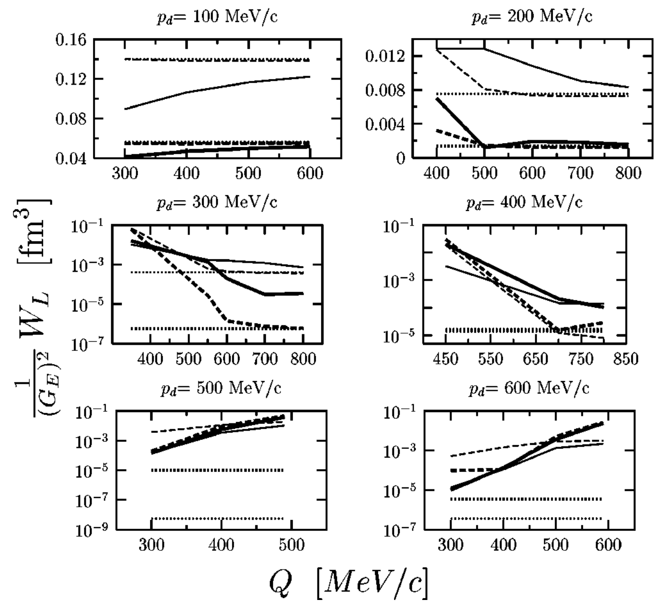

FIG. 5. $[1/(G_E)^2]W_L$ as a function of the three-momentum transfer Q for different p_d values. The curves correspond to PWIA (dotted line), PWIAS (dashed line), and Full (solid line) results. The thick curves are for the $M=\frac{1}{2}$, $M_d=0$, $m=\frac{1}{2}$ case, the thin lines for the $M=\frac{1}{2}$, $M_d=1$, $m=-\frac{1}{2}$ combination of the spin magnetic quantum numbers. In case of $p_d=400$ MeV/c the two PWIA results overlap.

and then to C_3. Symmetrization (PWIAS) has little effect at $p_d=10$ (not shown) and 100 MeV/c but has a big one for the smaller Q values in case of $p_d=200$–400 MeV/c and for all Q values in case of $p_d=500$–600 MeV/c. Rescattering plays mostly a strong role. In the case of C_1 ($p_d=10$ and 100 MeV/c) its effects are relatively small and diminish nicely with increasing Q. In the case of C_2 ($p_d=200$–400 MeV/c) its role is dramatic for $p_d=300$ and 400 MeV/c, which has to be expected since the proton and the deuteron travel together with a low relative energy $E_{3N}^{\mathrm{c.m.}}$. In the case of C_3 the two particles travel again opposite to each other as for C_1 and $E_{3N}^{\mathrm{c.m.}}$ decreases with increasing Q. In this case the by-far dominant contribution to the very strong deviation from the PWIA comes from antisymmetrization in the final state and FSIs leads to a relatively mild modification in case of $m=\frac{1}{2}$ but a significantly larger one for $m=-\frac{1}{2}$. Thus we see quite different outcomes depending on the cases and these theoretical predictions would be very interesting to be compared to data.

In case of W_T and $W_{T'}$ the spin operator appears in the current and moreover one can see the effects of the π- and ρ-like MECs. Nevertheless, the situation for $[2m_N^2/Q^2(G_M)^2]W_T$ shown in Fig. 6 is roughly spoken similar to the one for $W_L/(G_E)^2$. (We regard only W_T but of course $W_{T'}$ carries the same information.) Additionally one observes the effects of MECs, which are pronounced for $p_d=$ 300 and 400 MeV/c.

In view of all that, can we identify kinematic regions to pin down the spin dependent momentum distributions using W_L or W_T? We choose the cases of the closest approach of

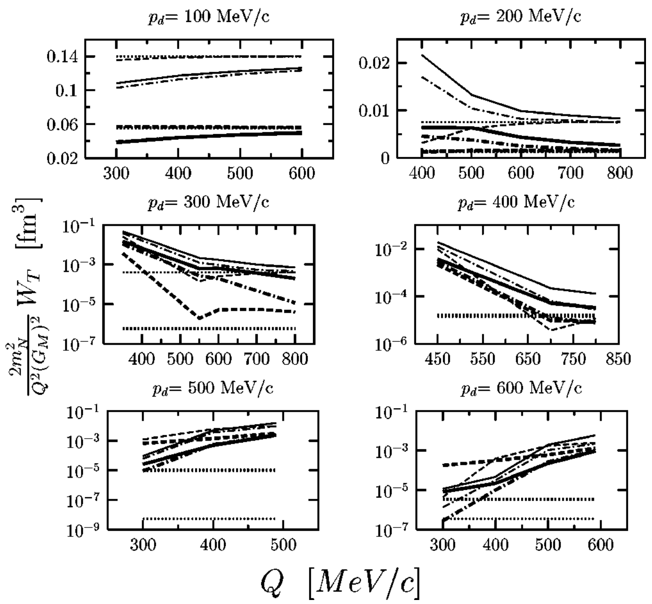

FIG. 6. $[2m_N^2/Q^2(G_M)^2]W_T$ as a function of the three-momentum transfer Q for different p_d values. The curves correspond to PWIA (dotted line), PWIAS (dashed line), Full without MEC (dash-dotted line), and Full including MEC (solid line) results. The thick curves are for the $M=\frac{1}{2}$, $M_d=0$, $m=-\frac{1}{2}$ case, the thin lines for the $M=\frac{1}{2}$, $M_d=1$, $m=\frac{1}{2}$ combination of the spin magnetic quantum numbers. In case of $p_d=400$ MeV/c the two PWIA results overlap.

PWIA and "Full" calculations (with MECs in case of W_T) for the different p_d values. They are displayed in Figs. 7 and 8 together with the spin dependent momentum distributions $\mathcal{Y}$ from Fig. 2. In case of $m=1/2$ the values of closest approach extracted from W_L and W_T differ for the larger q_0 values, where they also do not reach $\mathcal{Y}$. Only to the left of the zero of $\mathcal{Y}$ do they agree with each other and with $\mathcal{Y}$. For $m=-1/2$ the predictions for W_L and W_T agree with each other but do not show the strong dip of $\mathcal{Y}$. For the smaller q_0 values they agree with $\mathcal{Y}$. As a consequence of these results the asymmetry A formed out of those values of closest approach cannot follow the asymmetry formed out of the $\mathcal{Y}$'s. Only the values extracted for W_L show a mild similarity with the asymmetry A, as shown in Fig. 9.

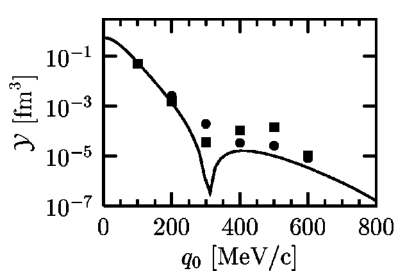

FIG. 7. $\mathcal{Y}(M=\frac{1}{2},\ M_d=0,\ m=\frac{1}{2};\ q_0)$ (solid curve) as a function of the relative proton-deuteron momentum q_0 together with the values of closest approach (see text) from W_L (squares) and from W_T (circles).

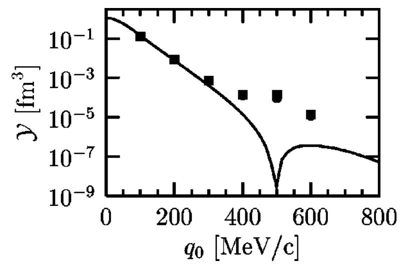

FIG. 8. $\mathcal{Y}(M=\frac{1}{2},\ M_d=1,\ m=-\frac{1}{2};\ q_0)$ (solid curve) as a function of the relative proton-deuteron momentum q_0 together with the values of closest approach (see text) from W_L (squares) and from W_T (circles).

IV. SUMMARY

Based on the NN force AV18 and consistent π- and ρ-like exchange currents we investigated within the Faddeev framework the process $\overrightarrow{^3\mathrm{He}}(e,e'\vec{p})d$ [or $\overrightarrow{^3\mathrm{He}}(e,e'\vec{d})p$]. The aim was to have access to the spin dependent momentum distribution of polarized $\vec{p}\vec{d}$ clusters in polarized ^{3}He. That distribution would provide interesting insight into the ^{3}He wave function. We restricted ourselves to a nonrelativistic regime, where the $3N$ c.m. energy of the final state should stay below the pion threshold. In that kinematical regime we explored the longitudinal and transverse response functions W_L and W_T, as well as $W_{T'}$, as a function of the final deuteron and the allowed photon momenta. All the spins and momenta are chosen parallel or antiparallel to the photon momentum. While in the PWIA W_L and W_T ($W_{T'}$) up to known factors yield directly the sought spin dependent momentum distribution, FSIs and MECs preclude in most cases the direct access to that distribution. The response functions W_L and W_T multiplied by appropriate factors have been mapped out in a wide kinematical range and this theoretical outcome should be checked experimentally. It presents the present day state-of-the-art insight into the dominant photon absorption process and the few-nucleon dynamics. It is only at small deuteron momenta $p_d \leqslant 2$ fm^{-1} that the investigated momentum distribution can be accessed within the constrained kinematics we have chosen.

Right now we have no reliable estimate for the amount of relativistic corrections or insight into the stability of our results under exchange of nuclear forces and consistent MECs. Clearly work in that respect should be envisaged.

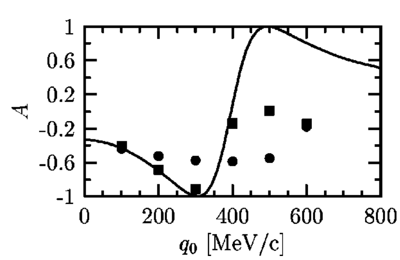

FIG. 9. The asymmetry $A=[\mathcal{Y}(m=\frac{1}{2})-\mathcal{Y}(m=-\frac{1}{2})]/[\mathcal{Y}(m=\frac{1}{2})+\mathcal{Y}(m=-\frac{1}{2})]$ as a function of the relative proton-deuteron momentum q_0 together with the values of closest approach (see text) from W_L (squares) and from W_T (circles).

ACKNOWLEDGMENTS

We are indebted to Dr. H. Gao and Dr. D. Dutta, who inspired us to perform this study. We would also like to thank Dr. M. O. Distler for an interesting discussion about experiments with polarized electrons. This work was supported by the Deutsche Forschungsgemeinschaft (J.G.), the Polish Committee for Scientific Research under Grant Nos. 2P03B02818 and 2P03B05622, and by NFS Grant No. PHY0070858. R.S. acknowledges the Foundation of Polish Science for financial support. The numerical calculations have been performed on the Cray T90 of the NIC in Jülich, Germany.

[1] J. L. Forest, V. R. Pandharipande, Steven C. Pieper, R. B. Wiringa, R. Schiavilla, and A. Arriaga, Phys. Rev. C **54**, 646 (1996).

[2] R. B. Wiringa, V. G. J. Stoks, and R. Schiavilla, Phys. Rev. C **51**, 38 (1995).

[3] W. Glöckle, *The Quantum Mechanical Few-Body Problem* (Springer-Verlag, Berlin, 1983).

[4] T. W. Donnelly and A. S. Raskin, Ann. Phys. (N.Y.) **169**, 247 (1986).

[5] J. Golak, H. Kamada, H. Witała, W. Glöckle, and S. Ishikawa, Phys. Rev. C **51**, 1638 (1995); J. Golak, H. Witała, H. Kamada, D. Hüber, S. Ishikawa, and W. Glöckle, *ibid.* **52**, 1216 (1995); S. Ishikawa, J. Golak, H. Witała, H. Kamada, W. Glöckle, and D. Hüber, *ibid.* **57**, 39 (1998); J. Golak, G. Ziemer, H. Kamada, H. Witała, and W. Glöckle, *ibid.* **63**, 034006 (2001).